



Size Effect on The Shear Strength of Reinforced Concrete Beams

Hind T. Jaber*, Kaiss F. Sarsam, Bassman R. Muhammad 

Civil Engineering Dept., University of Technology-Iraq, Alsina'a street, 10066 Baghdad, Iraq.

*Corresponding author Email: hindalmgoter@gmail.com

HIGHLIGHTS

- Increasing beam cross-section size from (75x150) mm to (150x300) mm has decreased the ultimate shear stress with different ratios.
- The percentage of decrease was 8, 12 for concrete compressive strength of 45MPa and tensile steel reinforcement ratio of ($\rho/\rho_b = 0.18$).
- The percentage of decrease was 9, 7 and 9 for concrete compressive strength of 65MPa and tensile steel reinforcement ratio of ($\rho/\rho_b = 0.18$).

ABSTRACT

According to research, as the depth of a beam increases, the section's shear strength can be expected to decrease. The size effect is a phrase that has been used to describe this tendency. Testing of unreinforced specimens under shear has also shown that the shear strength might be lower than what is typically anticipated in the design. As a result, it is critical to comprehend the behavior of these structures, as they may be influenced by a size impact. Sixteen reinforced concrete beams of different rectangular cross-sections without stirrups were tested. The tested beams were simply supported made of high-strength reinforced concrete subjected to two equal concentrated loads up to the failure. The experimental results showed that all of the beam specimens failed in shear except one which had failed by flexure. Moreover, increasing beam height from 150 to 250 mm has decreased the cracking and ultimate shear strength ratio for all groups except for group four when the beam height increased from 150 to 300 mm the cracking and ultimate shear strength ratio has increased. Furthermore, increasing beam depth from 150mm to 300mm has led to increasing the ultimate load besides decreasing their final deflection at the same level of load, which is the apparent size effect in the stiffness of the tested beams.

ARTICLE INFO

Handling editor: Wasan I. Khalil

Keywords:

Cracking
Deflection
High Strength Concrete
Shear Strength
Slender Beams
Size Effect

1. Introduction

The development of large-scale reinforced concrete (RC) structures, such as high-rise skyscrapers, long-span bridges, and nuclear power plants, has grown dramatically in recent decades. The cross-sections of members expand when the constructions become taller and larger in scale. These massive components necessitate an excessive amount of concrete and steel reinforcement, resulting in a hefty self-weight and costly structure. Many investigators have been interested in finding ways to better employ high-strength materials in order to minimize excessive use of building materials and have performed numerous research studies. Among these, research on the material characteristics of high-strength concrete, structural analysis, and design technology, and its suitability as a building material has progressed to a mature level of knowledge[1][2]. Because of the concrete brittle nature, shear failure in these members is difficult to anticipate and govern, that is why they are typically avoided at all costs. The majority of shear failures in RC members are caused by concrete bending cracks, which make the member vulnerable to significant shear stresses and flexural-shear failure[3].

2. Literature review on size effect

Cholostiakow et al. [3] investigated experimentally the size effect on the shear behavior of fiber-reinforced-polymer (FRP) RC beams with and without shear reinforcement and overall depth varying from 260 to 460 mm. A total of fifteen simply supported specimens were tested in an asymmetric 3-point bending configuration. The main parameters were effective depth, d ; the presence of shear links; and concrete strength. All other parameters, including beam width, longitudinal tensile reinforcement ratio, and shear-span-to-depth ratio were kept constant. The results confirmed a considerable size effect for

1960

members without shear reinforcement, showing an average reduction in normalized shear strength of about 19 %, with a maximum value of up to 40 %. Furthermore, current design provisions are overall conservative, but with non-uniform margins of safety that decrease with increasing member depth. Current FRP design equations do not predict the shear strength of FRP RC beams of different sizes with a uniform margin of safety. You and Yang, 2018[4] studied the effectiveness of steel fibers and a minimum number of stirrups on the shear response of various sized reinforced HSC beams. Six large reinforced High Strength Concrete (HSC) beams with a shear span-to-depth ratio of 3.2 and a longitudinal steel reinforcement ratio of 0.03 were manufactured. Three of them contained 0.75% (by volume) steel fibers without stirrups, while the rest were reinforced with the minimum number of stirrups without fibers. The study used three different section sizes: 300 x 500mm, 450 x 750mm and 600 x 1000mm. Test results indicated that, with increasing beam size, significantly lower shear strength was obtained for steel fiber-reinforced high-strength concrete beams without stirrups, than for the plain HSC beams with stirrups. On the other hand, the use of minimum stirrups gave better shear cracking behaviors than that of steel fibers and effectively mitigated the size effect on shear strength.

Lee et al. [5] examined sixteen large-scale RC beams to see if high-strength stirrups could be used on the specimens under shear failure. The study used four different section sizes: 500 x 600 mm, 500 x 850 mm, 500 x 1100 mm, and 500 x 1350 mm. For the stirrups, two various grades of steel, Grade 60, and Grade 80, were used to make out the beam specimens. The shear span depth ratio was designed to be 2.5 and the tensile reinforcement ratio was 1.61% in all specimens. The test results showed that as the cross-section size increased, the normalized ratio for beams without shear reinforcement decreases. Moreover, the cross-section depth was related to the ultimate shear strength. Finally, when the cross-section depth increased and the stirrup ratio decreased, the inclination angle of diagonal cracks decreased. Althing and Lippi, [6] studied the effect of size on the shear capacity for RC beams with and without stirrups. A total of 16 simply supported RC specimens were tested less than one point load till failure. Four different cross-section sizes were chosen namely, A (160 x 200 mm), B (160 x 250 mm), C (160 x 300 mm), and D (100 x 150 mm). The shear span to the effective depth ratio, reinforcement ratio, and concrete compressive strength were held constant. The test result indicated that, except for the cross-section class D, the average nominal stress reduces with increased beam depth for both with and without web reinforcement beams, indicating that a size impact existed in the smaller beams. Moreover, as the beam height was increased from 200 to 300mm, the ratio between tested and predicted shear capacity exhibited a general increasing (declining) trend in the shear (non-shear) RC beams. Shin et al.[7]studied the shear behavior of RC beams having high-strength stirrups with large-size cross-section sections. The size of the cross-section, yield strength of the stirrups, and web reinforcement ratio were the main parameters for the 19 beam specimens. Two series of experiments were carried out. Eleven RC beams with four dissimilar cross-sections were chosen for the first set of experiments: 490 x 600 mm, 495 x 900 mm, 480 x 1200 mm, and 540 x 1500 mm. Meantime, the second set of experiments used eight RC beam specimens with two various cross-sectional sizes: 500 x 850 mm and 500 x 1100 mm. The shear span to effective depth ratio and tensile reinforcement ratio was designed to be 2.5% and 1.53%, respectively for all specimens. According to experimental data, the shear strength ratio of specimens reduces as the cross-sections size of RC beams increases, independent of whether the beam was reinforced with plane-strength or high-strength reinforcing steel bars. Furthermore, as the depth of the beam and the amount of web reinforcement increased the difference between tests and predicted shear strength dropped. Moreover, the load-deflection relation of specimens indicated that as beam size increased, the strength and mid-span deflection of the beam specimens increased as well, owing to the increased shear contribution of concrete. Jumaa and Yousif, et al.[8] Studied and tested the effect of size in the shear failure of twelve large-scale HSC beams without web reinforcement, reinforced with basalt fiber reinforced polymer bars under two point's loads. The main variables were beam depth (from 300 to 700 mm), flexural reinforcement ratio (ρ) (from 0.706 to 2.069 %), and concrete compressive strength (42.2 and 73.4 MPa). When the beam depth was changing from 252 to 452 and 635 mm, respectively, the test results showed a significant size effect on normalized shear strength, with average decreases in shear strength of 32.8 and 43.6 percent. Additionally, in beams with low tensile reinforcement, the size effect was greater. The maximum deflection and ductility of a beam decrease as its depth increases, and the failure mode becomes more brittle. In another conclusion, there was no considerable impact in size effect between normal strength concrete (NSC) and high-strength concrete beams, with the size influence in NSC beams being slightly greater than that in relating to HSC beams. Wu et al., [9]investigated the shear behavior and size impact of fifteen concrete deep beams. Beam depths (500 to 1400 mm), shear span-depth ratios (a/d) (0.75, 1, and 1.5), and bearing plate widths (130 and 200 mm) were the test parameters. All beam specimens had a constant width of 180 mm also the web reinforcement ratio was kept constant. According to the findings, all specimens failed in shear-compression mode. The mode of failure for each specimen was largely unaffected by beam depth variation, while and had a significant impact. When beam height was increased from 500 to 1400 mm, the normalized shear strength at failure dropped by roughly 37.1 percent, demonstrating considerable size dependency. The influence of beam depth on normalized cracking shear stresses, on the other hand, may be ignored. Chao, [10] investigate the effect of size on steel fiber-reinforced concrete (SFRC) slender beams. The experiments were conducted out on a set of SFRC beams with heights ranging from 305 to 1220 mm. Twelve beams were examined, including five pairs of SFRC and one pair of 457 mm deep RC beams. Shear span to effective depth ratio, longitudinal reinforcement ratio, steel-fiber volume percentage, type of fiber, and concrete strength were all kept constant for all beam specimens. The findings were unique in that they contradicted the traditional theory by correlating the size effect of ultimate shear strength on SFRC beam specimen to the effects of the dowel resistance and compression zone, rather than simply lowering aggregate interlock or fiber bridging capacity in bigger SFRC beams due to a larger critical crack. As a result, a weaker dowel zone, such as one with poorly distributed steel fibers or insufficient fiber dose, can lead to early dowel resistance failure and subsequent shear failure, amplifying the size impact. Furthermore, when the total beam depth is increased from 305 to 1220 mm, the ultimate shear strength decreases by 25%.

3. Problem Statement

Considering all of the preceding studies on the influence of beam size on the shear strength of RC structures are taken into account, there is evidence indicating as the beam's depth increases, the section's shear strength decreases. The size effect is a phrase that has been used to describe this tendency. Shear testing of unreinforced specimens has also shown that shear strength might be lower than typically anticipated in the design. To reveal more of these deficiencies, and according to all works mentioned previously, few studies had been done to examine the size effect on high-strength RC beams without shear reinforcement. As a result, it is critical to comprehend these structures' behavior, as they may be influenced by the size impact, consequently, this study had been conducted.

4. Material used

4.1 Cement

Throughout the experimental work of this study, Ordinary Portland Cement (Type I) manufactured by the united cement company in Iraq was used to prepared high-strength concrete mixes. The cement chemical analysis and physical test were made at the National Center of Construction Laboratories and Research and the test results showed that the adopted cement conformed to the Iraqi specification No. 5/1984 [11].

4.2 Fine Aggregate

Al-Ukhaider natural sand with a smooth texture of 2.85 as a fineness modulus and rounded particle form was used. The fine aggregate grading and the physical properties test were made in the National Center for Construction Laboratories and Research and the test results showed that the fine aggregate was used within the requirements of the Iraqi Specification No. 5/1984[11].

4.3 Coarse Aggregate

Throughout the tests, the maximum crushed gravel size in the concrete mixes was limited to 9.5 mm. According to Taylor, [12], the maximum aggregate size has an effect on the mechanism of interface shear transfer, concrete shear strength is somewhat reduced as the maximum aggregate size decrease. To achieve a workable lower bound on the aggregate size effect on the shear strength of the concrete, a comparatively small maximum aggregate size in the concrete patches were utilized. Before use; the crushed coarse aggregate was washed, dried in the air, and then kept in a saturated dry surface state. The coarse aggregate specific gravity and absorption were 2.6 and 0.66%, respectively. The coarse aggregate grading was performed in the Construction Materials Laboratory at the University of Technology and the test results showed that the coarse aggregate used was within the requirement of the Iraqi specification No. 5/ [11].

4.4 Super plasticizer

Sitka chemical construction's Sika-viscocrete® -5930L was used as a high-range water-reducing admixture during the production of the concrete mixes to reduce the water-cement ratio, make concrete placement easier, and enhance the mix's workability. This kind of super plasticizer can be used with any type of Portland cement that meets recognized international standards. The properties of the superplasticizer used that supplied by the manufacturer was confirmed with the requirement of ASTM C-494/C494M Types A and F[13].

4.5 Silica Fume

The mixture of concrete included Mega Add MS (D) concentrations silica fume developed by MSASA construction chemical manufacturer. Silica fume is a fine powder pozzolanic substance with particles that are 100 times smaller than cement particles. It is used in a small amount or as a partial substitute for cement to improve concrete characteristics including concrete permeability and its strength. The silica fume chemical composition test results was conformed to the requirements of the ASTM C1240-05 [14].

4.6 Water

Clean potable water from the water-supply network system was used for both mixing and curing of concrete specimens.

4.7 Steel Reinforcement

Deformed steel bars with four nominal diameters of 8, 10, 12, and 16mm were used as beams flexural main reinforcing bars in tension, while in order to evaluate the shear strength provided by the concrete, no web reinforcing bars were used in any of the beam specimens. To determine the yield and ultimate tensile strengths, tensile tests were conducted on representative coupons of the steel bars. The tension tests of the bar specimens were conducted at the Laboratory of Material Resistance at the University of Technology. The test results of bars used in the experimental work satisfy the ASTM A615-16[15]requirements.

5. Concrete Mixture Proportions

Two-target concrete mixture, several trial mixes for each targeted concrete compressive strength were done to determine the distinctive cylinder concrete compressive strength of (45 and 65) MPa at 28 days. The cylinder compressive strength test

was performed according to American stranded specification ASTM C39/C39M-03[16]. For each concrete mix, the cylinder dimensions used were 100 mm for diameter and 200 mm for height. Table1 shows a detailed description of the concrete mixture component that was employed in this study.

Table 1: Concrete mixture components

Mix Strength	Mix Design						face (MPa)		Average face at 28 days (MPa)
	Cement/ m^3	Sand kg/m^3	Gravel kg/m^3	Silica fume kg/m^3	W/C	SP. by weight of cement	at 7 days	at 28 days	
45 MPa	460	800	1000	45	0.32	0.04	32.06	45.56	44.73
							34.18	48.57	
							28.18	40.04	
65 MPa	637	561	993	71	0.22	0.04	43	61.10	66.65
							51	72.47	
							46.7	66.36	

6. Experimental Program

The experimental program consists of cast and tests sixteen reinforced concrete beams of different rectangular cross-sections. The tested beams were simply supported made of high-strength reinforced concrete subjected to two equal concentrated loads up to the failure. All the reinforced concrete beams were without web reinforcement, and they all designed to evaluate the specimens' shear behavior. Table 2 summarizes the beam specimens' details and material properties. The cross-section size of the specimens is the most important parameter. In this investigation, four distinct section sizes were used: (75x150 mm), (100x200 mm), (125x250 mm), and (150x300 mm) with a constant length of 1600 mm which were cast in a wood form, see Figure 1. According to the cross-section sizes, test specimens are divided into four groups (BA, BB, BC, and BD), with each group consisting of four specimens. The main adopted parameters are the concrete compressive strength (45 and 65 MPa) and the tensile reinforcement ($\rho/\rho_b = 0.18$ and $\rho/\rho_b = 0.28$). There was no web reinforcing in any of the specimens used to determine the nominal shear strength of concrete but a stirrup with a diameter of 6 mm was used only at the ends for all the beam specimens to fix and to protect the cushions from failure during loading and inspection. The longitudinal reinforcement ratio was designed to be from (0.00503 to 0.01408) as relatively high to prevent flexural failure before shear failure. The tensile steel ratio in the tested beams was less than the balanced steel ratio and, therefore, all the beams were designed to be under reinforced. The longitudinal steel was distributed evenly over the specimens' width, leaving a 10mm concrete cover on either side. The bottom cover was chosen in accordance with ACI 318M-19 [17] for 15mm internal exposed beams. To eliminate the danger of anchoring failure, the bottom main steel bars were hooked upward beyond the supports. The shear design formulae in ACI 318M-19[17] were used to design all of the specimens.

Table 2: Details of specimens and material properties

Group No.	Specimen Notation*	Cross Section			Shear to Span	Comp. Strength	Longitudinal Tensile Reinforcement		
		b (mm)	h (mm)	d (mm)			a/d	f_c (MPa)	ρ/ρ_b
BA	BA75*150-45-(3-8)	75	150	125	4.48	45	0.18	3Ø8	420
	BA75*150-65-(3-8)	75	150	125	4.48	65	0.18	3Ø8	420
	BA75*150-45-(4-8)	75	150	113	4.96	45	0.28	4Ø8	420
	BA75*150-65-(4-8)	75	150	113	4.96	65	0.28	4Ø8	420
BB	BB100*200-45-(2-10)	100	200	174	3.22	45	0.18	2Ø10	513
	BB100*200-65-(2-10)	100	200	174	3.22	65	0.18	2Ø10	513
	BB100*200-45-(3-10)	100	200	174	3.22	45	0.28	3Ø10	513
	BB100*200-65-(3-10)	100	200	174	3.22	65	0.28	3Ø10	513
BC	BC125*250-45-(2-12)	125	150	223	2.52	45	0.18	2Ø12	513
	BC125*250-65-(2-12)	125	150	223	2.52	65	0.18	2Ø12	513
	BC125*250-45-(3-12)	125	150	223	2.52	45	0.28	3Ø12	513
	BC125*250-65-(3-12)	125	150	223	2.52	65	0.28	3Ø12	513
BD	BD150*300-45-(2-16)	150	300	271	2.07	45	0.18	2Ø16	530
	BD150*300-65-(2-16)	150	300	271	2.07	65	0.18	2Ø16	530
	BD150*300-45-(3-16)	150	300	271	2.07	45	0.28	3Ø16	530
	BD150*300-65-(3-16)	150	300	271	2.07	65	0.28	3Ø16	530

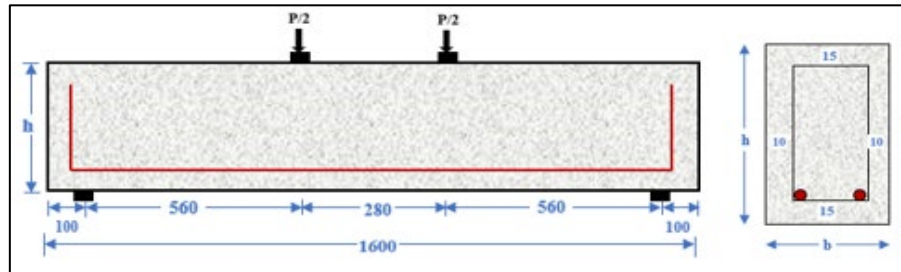
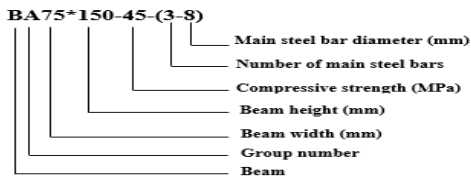


Figure 1: Beam cross-section details (Note: all dimensions in mm)*Beam Notation

7. Mixing Casting Procedure

In this study wooden molds were used to fabricate beam specimens with four different dimensions of inner dimensions (75, 100, 125, and 150) mm in width, (150, 200, 250, and 300) mm in depth, and 1600 mm in length. The steel reinforcement cages were placed in its required place in the mold after cleaning, oiling inner faces, and fastening the parts of it. The concrete mixing was done in a tilting rotary mixer 0.19 m³ capacity. The required materials were weighted and stored according to the specified percentages as previously stated prior to mixing the component in the following order:

The silica fume powder was mixed with the cement in a dry state using a tilting rotary mixer with a mixing speed of roughly 15 rpm for approximately four minutes to ensure that the silica fume powder was fully distributed between cement particles. Then the fine and coarse aggregates were added to the mixture to combine all the components together for around five to six minutes. The water and super plasticizer were then mixed together, and the solution was divided in half and mixed for ten minutes. One batch takes around half an hour to mix until it reaches the required consistency. Following completing the material mixing procedure, the mixture was poured into the wood molds in three layers, with each layer being compacted by an internal vibrator to achieve the concrete mixture's consolidation. The top surface of the specimens was then finished using a steel trowel. All specimens were kept in the laboratory for 24 hours after casting under polythene sheets, then marked and maintained in water container tanks until they reached the age of 28 days to be cured with almost constant laboratory temperature. Afterward, they were removed out of the tanks and maintained in the open at laboratory temperature for around 14 days before being tested. Before testing, all beam specimens were coated with white paint so that cracks could be clearly seen and photographed. The production, casting, and curing steps of concrete were according to the ASTM C192/C1 92M -05 [18]specification.

8. Test Instrumentations

Test specimens were instrumented to assess their behavior and strength in terms of load-deflection, crack pattern, and modes of failure. A number of instruments were installed on the tested beams to study their behavior during the loading process. These instruments are:

8.1 Electrical Resistance Strain Gauges

The strain gauge is one of the most significant tools for applying electrical measurement techniques to mechanical quantity measurement; it is used to measure the strain. In the present study, uniaxial electrical resistance (foil) strain gauges with a resistance of (120 ohms) were used to measure strains of the main reinforcement steel in the mid-span for the tested beams at different loading stages. Strain gauge-type steel electric strain gauges made by the Japanese company (TML) [19][FLA-6-11-3LJC] were installed in all beams.

8.2 Data Logger

The data logger KYOWA was used to read the strain gauges and linear variable differential transformer (LVDTs). The strain readings were recorded to excel data sheets using a software program once the data logger was linked to a computer.

8.3 Microcomputer Control Electronic Universal Testing Machine

Fifteen RC beams were tested by a WDW of 200 kN maximum capacity microcomputer control electronic universal testing machine that has the computerized controllability of the displacement applying. The test for fifteen beam specimens has been performed at the Department of Production Engineering and Metallurgy, Laboratory of Material Resistance at the University of Technology.

8.4 Hydraulic Universal Testing Machine

One reinforced concrete beam was tested using hydraulic universal (Avery Denison) testing machine of 2500 kN maximum capacity due to its higher expected failure loads which exceed the maximum capacity of the microcomputer control electronic universal testing machine (200 kN maximum capacity). This machine is present at the Civil Engineering Department's structural laboratory at the University of Technology.

9. Testing Procedure

Beam specimens were put on the testing machine and adjusted such that the centerline of the supports, as well as the point loads, was in their correct positions. Then, the concrete and steel strain gauges wires and the LVDTs were linked to the data logger. The beams were tested as simply supported beams over a clear span of 1400 mm under two equal point loads and the distance between the two concentrated loads remains constant at 280 mm. As the beam sets on two rollers support, the load was applied evenly on the tested beam at a distance of 560 mm from every support using a steel girder (HP 100×500× 40) mm with an overall length of (500 mm) which has been used to transport the load from the testing machine to the specimen through rectangular steel plates of (100 × 160 × 20) mm placed on the top of the beam to prevent local concrete crushing or bearing failure at both supporting positions and loading points. The width of the plates was slightly larger than the width of all beams. To provide uniform contact between the plates and the concrete specimens at the location of support plate and loading plate, a thin layer of rectangular rubber of (110 × 165 × 10) mm was used at each location.

9.1 Testing Using Microcomputer Control Electronic Universal Testing Machine

Firstly, a small amount of displacement (5 mm/min) was applied to seat the loading system and supports. After that, the strain gauge's initial readings through the data logger were taken to start the test with a rate of displacement (0.6 mm/min) for each beam up to ultimate deflection at failure.

The deflection readings at mid-span were recorded and monitored for each displacement increment using the computer program within the testing machine, strains in the steel reinforcement was also recorded and monitor during the test using personal computer connected to the data logger in selected displacement rate of (0.6 mm/min).

9.2 Testing Using Hydraulic Universal Testing Machine

Firstly, a small amount of displacement (2.5 kN) was applied to seat the loading system and supports. After that, the strain gauge's initial readings through the data logger were taken to start the test with a rate of loading (5 kN) for this beam up to ultimate load at failure. The deflection readings at misspent were recorded and monitored using linear variable differential transformer (LVDTs) connected to the data logger for each load increment during the test; strains in the steel reinforcement were also recorded and monitor during the test using personal computer connected to the data logger in selected load rate of (5 kN).

10. Results and discussions

10.1 General behavior and crack development

All of the tested beam specimens except one failed in shear when the ultimate strength was achieved prior to the strain gauges on the tensile reinforcements reached yield strain. However, it is only beam specimen BA75*150-65-(4-8) that had failed by the crushing of the compression zone at mid-span. The high compressive strength of concrete in this beam caused a much higher strength in shear than in bending which eventually led to bending failure. The beams were free of cracks in the early phases of loading. On one side of every beam specimen, flexure and shear cracks were examined and noted at load increment commencing from first application of load till failure. Flexural cracks were first appeared between loading points in the section of the pure flexural moment. As the load is increasing, further flexural cracks appeared in the area of the maximum moment. With furthers load, the cracks growth was seen to slow down and, in some cases, entirely stopped. In other situations, inclined shear cracks accompanied these flexural cracks resulting in flexure-shear cracks type. In most cases when the applied load was close to its maximum value, a main inclined shear crack began to widen up as a diagonal crack in the shear span region between the load and support point. It trends to the loading points downward along with the tensile steel reinforcement, generating localized splitting toward the support. Localized de-threading along the length of the tensile steel reinforcement occurred in the majority of the specimens, as evidenced by the existence of localized horizontal splitting cracks within the shear span; see representative specimens of the crack pattern of all beams in Figure 2, in which typical shear cracks are clearly seen. Other shear-critical specimens showed similar crack patterns following failure to Sneed Ramirez[20]beam's specimen failure mode. It can be concluded from the crack pattern of all beam spacemen's that with increasing shear span to depth ratio and beam height, the first diagonal crack location moved closer to the shear span's interior edge. Because none of the specimens had shear reinforcement, following the appearance of these diagonal cracks, the visible crack width increased without the number of cracks increasing because no more stress had been transferred to the stiffer parts, and all the tested beams collapsed suddenly after one or two large diagonal cracks had occurred. Shear-critical slender reinforced concrete members without web reinforcement are widely known for exhibiting a single diagonal crack accompanied by brittle shear failure. The load was increased slightly following the development of the diagonal cracks. Furthermore, once further diagonal cracks appeared, the load was rapidly reduced, as demonstrated in the load-deflection curves of the tested beams in the next paragraph. The width of the estimated diagonal crack was roughly proportionate to the size of the cross-section. Despite this,

several cracks were nearly steady. No major diagonal cracks were found before or during the failure of beam specimen BA75*150-65-(4-8), which failed by the crushing of the compression zone at mid-span (bending failure). Existing flexural cracks at mid-span expanded upwards to the loading plate, resulting in a significant increase in deflection upon failure, followed by crushing failure at the top surface of the beam specimen because the concrete compressive strength used was high in comparison to the steel low quantity. Therefore, the beam specimen BA75*150-65-(4-8) will be out of all the comparisons and discussions in this study. Despite the differences in total beam heights, Figure 2 shows that the width of the flexural crack along the longitudinal axis of the beam examined at the level of the tensile steel reinforcing bar was nearly similar in all the tested beams. To put it another way, the spacing of flexural crack measured at the tensile steel reinforcement level did not vary as the beam height increased. It was observed that the crack roughness decreased noticeably as the concrete strength increased. Also, it can be noted that no substantial flexural cracking, as well as no concrete crushing at misspent in the compression zone, was found in the specimens of group BD, which represents the larger group in size. These specimens developed a large diagonal crack after further deformation, resulting in shear failure. Furthermore, larger beams demand less stress at the crack tip for further crack propagation, according to Bezzant's size-effect equation [21],[22]. As a result, larger beams have a less explosive failure mode. Regardless of the lack of precision in estimating the associated load; the start of the inclined fracture indicates a significant shift in the behavior of the beam without shear reinforcing. The start of the inclined crack did not cause the beams in this research to collapse immediately. Many different studies have noticed this phenomenon, which is detailed in ACI-ASCE 445[23], where the beginning of an inclined crack leads to a complicated redistribution of forces that alters the contributions of the various shear transfer mechanisms.

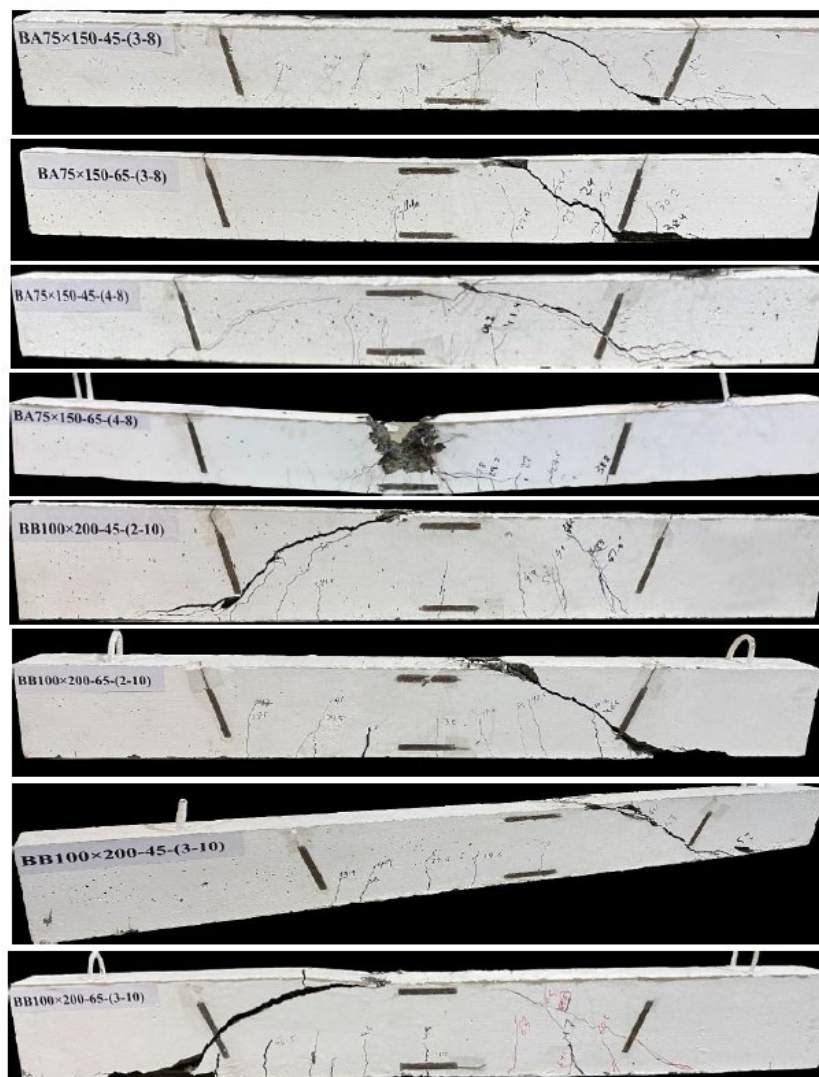


Figure 2: Crack patterns after failure



Figure 2 Continued

10.2 Cracking and Ultimate capacity

The cracking load, ultimate load with their corresponding deflection as well as the type of failure mode for all the tested beams are listed in Table 3. Except for beam BA75*150-65-(4-8), smaller beams typically withstand higher ultimate shear

stress at failure than bigger beams, indicating that the size of beam has apparent influence on its shear strength. It should be noted that the beam specimen BA75*150-65-(4-8) has the least increasing ratio in failure load for each increase of concrete compressive strength and steel reinforcement ratio, this is related to its failure mode which is different from all the other 15 reinforced concrete beams in the testing program. Therefore, the beam specimen BA75*150-65-(4-8) will be out of all the comparisons and discussions in this study.

Table 3: Beam specimens test results

Group No.	Specimen Notation*	Pcr (kN)	Deflection at Pcr (mm)	Pu (kN)	Deflection at Pu (mm)	Observed Failure Mode
BA	BA75*150-45-(3-8)	20.93	5.2	33.44	9.908	Diagonal tension- shear failure at one side
	BA75*150-65-(3-8)	22.54	4.571	43.23	12.802	Diagonal tension- shear failure at one side
	BA75*150-45-(4-8)	25.52	5.414	45.48	13.654	Diagonal tension- shear failure at both side
	BA75*150-65-(4-8)	27.64	6.2	46.52	15.526	Crushing in the compression zone
BB	BB100*200-45-(2-10)	30.22	4.144	57.4	9.188	Diagonal tension- shear failure at one side
	BB100*200-65-(2-10)	32.8	4.647	73.17	11.277	Diagonal tension- shear failure at one side
	BB100*200-45-(3-10)	35.44	3.6	65.45	7.923	Diagonal tension- shear failure at both side
	BB100*200-65-(3-10)	37.04	3.827	83.94	11.029	Diagonal tension- shear failure at both side
BC	BC125*250-45-(2-12)	40.41	2.42	87.25	8.72	Diagonal tension- shear failure at one side
	BC125*250-65-(2-12)	45.65	3.121	120.1	11.956	Diagonal tension- shear failure at both side
	BC125*250-45-(3-12)	48.6	3.655	102.6	8.55	Diagonal tension- shear failure at one side
	BC125*250-65-(3-12)	66.1	4.728	157.3	13.424	Diagonal tension- shear failure at both side
BD	BD150*300-45-(2-16)	70.2	4.44	161.2	9.707	Diagonal compression-shear failure at both side
	BD150*300-65-(2-16)	95.3	6.67	171.2	10.8	Diagonal compression-shear failure at both side
	BD150*300-45-(3-16)	100.02	5.522	200.5	10.77	Diagonal compression-shear failure at both side
	BD150*300-65-(3-16)	125.4	3.267	285.1	7.011	Diagonal compression-shear failure at both side

10.3 Influence of Size on Cracking and Ultimate Capacity

As mentioned earlier in the literature review for the size effect and its influence on the shear concrete capacity, shear behavior of reinforced concrete slender beams with no shear reinforcement has demonstrated the importance of size effect on ultimate shear strength, as the beam depth increases, the ultimate shear stress at failure decreases. This means that, the results of small-scale beam tests do not apply to large-scale beams. The finding from tests by Shia et al. [24], Figure 3, is based on one of the most widely accepted justifications of the size impact on maximum shear strength for reinforced concrete beams. The average horizontal crack spacing, S, at mid-height of the beam was about half of the beam's effective depth, according to their findings. This led to the idea that as a slender beam gets deeper (that is, its "size"), the crack spacing will increase. The average crack width, W_x , is substantially proportional to the product of the average crack spacing and tensile steel reinforcing strain, as if the concrete elastic strain between two consecutive cracks are ignored [25]. As a result, an increase in beam size at a given main steel bar strain produces an increase in crack spacing, which leads to larger cracks, decreasing aggregate interlock capability in resisting shear [24][26]. According to this theory, if the beam size increases, the crack size increases too, any variable that produces an increase in either tensile strain in main steel reinforcement or crack spacing can result in crack width increasing and an aggregate interlock capability reduction, aggravating the size impact.

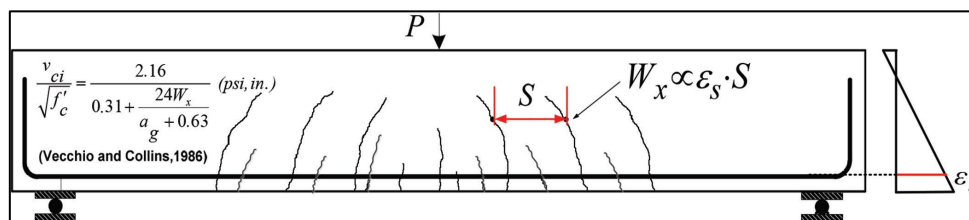


Figure 3: The hypothesis of size effect on ultimate shear strength [24]

Figure 4 represents the influence of size on the capacity of visible cracking and ultimate loads for all beam specimens with constant concrete strength (45MPa and 65MPa) and the same flexural reinforcement ratio (ρ/pb of 0.18 and ρ/pb of 0.28). The size influence on the reinforced concrete tested beams in terms of visible cracking and ultimate loads were the more important variable from the concrete compressive strength or the main reinforcement ratio.

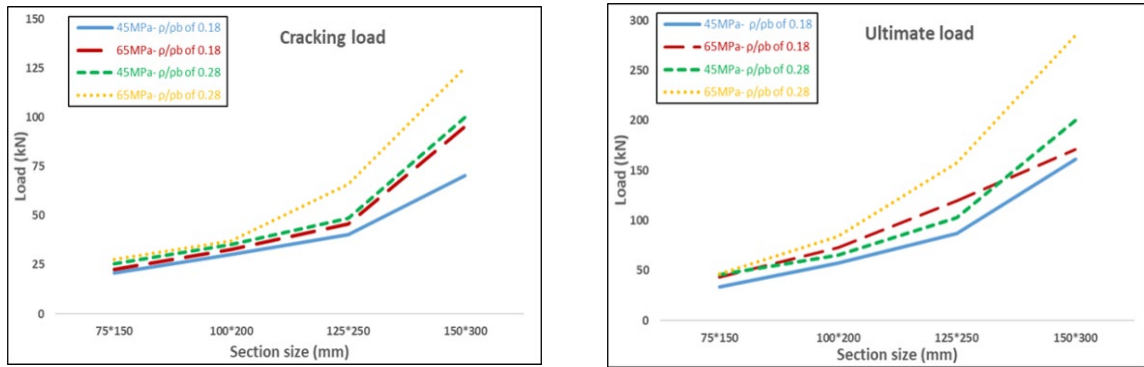


Figure 4: The capacity of cracking and ultimate load with varying cross-sections size

Table 4 shows the ratio of the visible cracking and ultimate strength for different cross-section sizes with constant concrete compressive strength (45MPa and 65MPa) and the same longitudinal reinforcement ratio (ρ/pb of 0.18 and ρ/pb of 0.28) for all tested beam specimens.

Table 4: Cracking and ultimate strength ratio per different beam size

Specimen	Pcr		Pu	
	$\frac{Pcr}{2bw d \sqrt{f'c}}$	$\frac{Pcr}{2bw d \sqrt{f'c}} \%$	$\frac{Pu}{2bw d \sqrt{f'c}}$	$\frac{Pu}{2bw d \sqrt{f'c}} \%$
BA75*150-45-(3-8) *	0.139	1.000	0.222	1.000
BB100*200-45-(2-10)	0.113	0.812	0.214	0.966
BC125*250-45-(2-12)	0.096	0.695	0.208	0.939
BD150*300-45-(2-16)	0.116	0.839	0.267	1.205
BA75*150-65-(3-8) *	0.124	1.000	0.238	1.000
BB100*200-65-(2-10)	0.102	0.819	0.227	0.952
BC125*250-65-(2-12)	0.091	0.729	0.238	1.000
BD150*300-65-(2-16)	0.131	1.057	0.236	0.990
BA75*150-45-(4-8) *	0.169	1.000	0.301	1.000
BB100*200-45-(3-10)	0.132	0.781	0.244	0.809
BC125*250-45-(3-12)	0.116	0.686	0.245	0.812
BD150*300-45-(3-16)	0.166	0.980	0.332	1.102
BA75*150-65-(4-8) *	0.152	1.000	0.256	1.000
BB100*200-65-(3-10)	0.115	0.754	0.260	1.015
BC125*250-65-(3-12)	0.131	0.861	0.312	1.217
BD150*300-65-(3-16)	0.173	1.134	0.393	1.532

* Reference beam to compare

In general, it can be seen from Table 4, that increasing beam height from 150mm for group BA to 300mm for group BD has influenced both the normalized first cracking load and ultimate shear capacity of the tested beam. Increasing beam height from 150 to 250 mm has decreased the shear strength with different ratios. The percentage of decreasing was 34, 61 for concrete compressive strength of 45MPa and ρ/pb of 0.18, 48, 0 for concrete compressive strength of 65MPa and ρ/pb of 0.18, and 191, 188 for concrete compressive strength of 65MPa and ρ/pb of 0.28. It can be concluded that increasing the beam depth increases the concrete contribution in the shear equation, which eventually leads to a decrease in the ultimate shear strength of the beam. It can be seen from Table 4, increasing beam height from 150 to 300 mm has increased the shear strength. The percentage of increasing was 205, and 102 for concrete compressive strength of 45MPa and 65MPa with ρ/pb of 0.18 and 0.28. In other words, the behavior of the group BD is different and, in some way, than other groups in terms of increasing beam depth on the shear capacity. This may be related to that beams in this group had an a/d ratio of 2.07 which is close to behaving

as a deep beam. With decreasing a/d , the effectiveness of arch action in deep beams is developed leads to enhance the concrete capacity of these beams. Consequently, results in increasing the shear strength with different ratios.

10.4 Influence of Concrete Strength on Cracking and Ultimate Capacity

The ultimate load P_u and the visible cracking load per of all tested beams increased significantly with an increase in concrete compressive strength (face), as expected. Figure 5 represents the effect of the concrete compressive strength on the capacity of visible cracking load P_{cr} and ultimate load P_u in each group for all beam specimens without stirrups with constant longitudinal reinforcement ratio (ρ/pb of 0.18 and ρ/pb of 0.28) and same cross-section (75*150mm, 100*200mm, 125*250mm and 150*300mm).

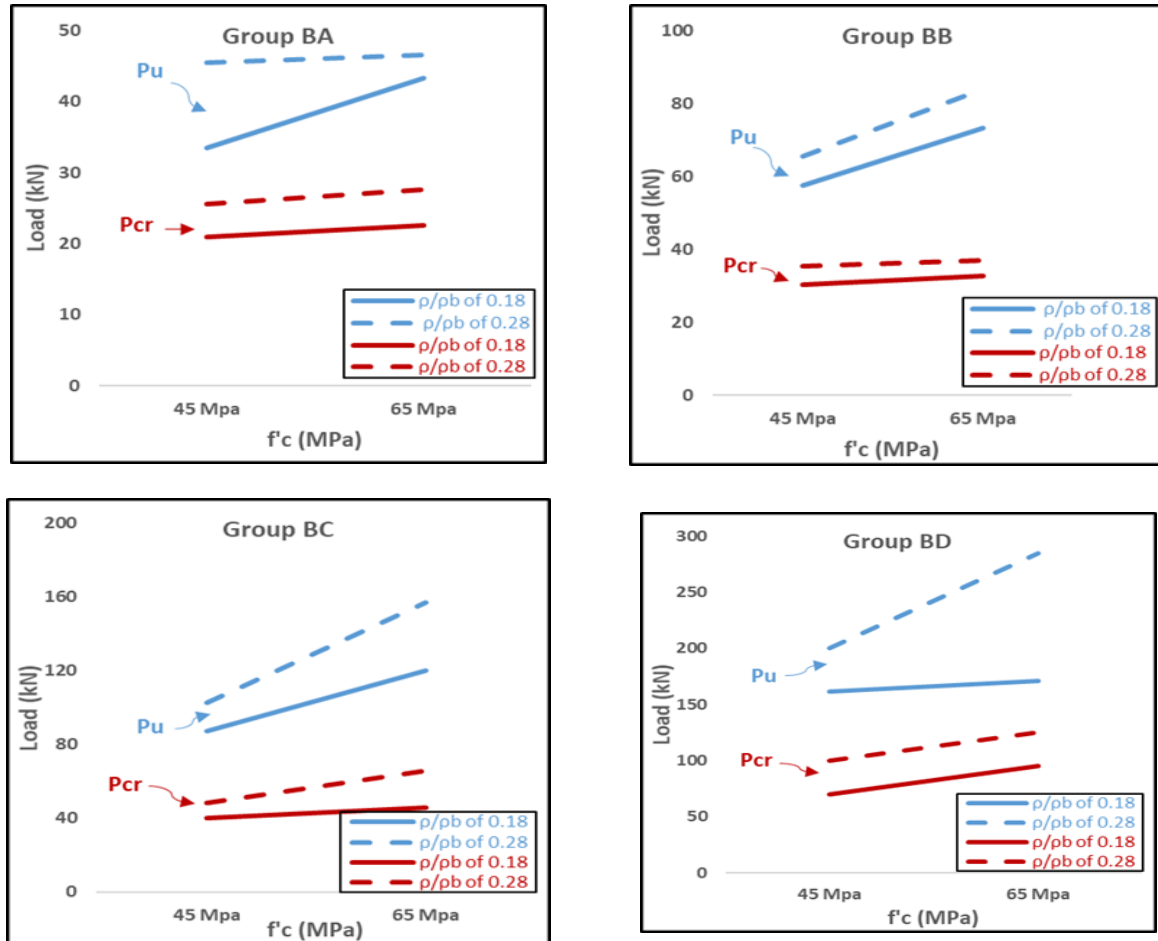


Figure 5: Capacity of cracking and ultimate loads with varying concrete compressive strength

Table 5 shows the increasing percentage of the visible cracking and ultimate loads for different concrete compressive strengths with constant cross-section sizes (75*150mm, 100*200mm, 125*250mm and 150*300mm) and the same longitudinal reinforcement ratio (ρ/pb of 0.18 and ρ/pb of 0.28) for all tested beam specimens.

Table 5 illustrates this, the increasing the of concrete compressive strength from 45 MPa to 65 MPa, increases the ultimate shear strength for all groups. The percentage of increase was different for each group and depending on the amount of steel reinforcement ratio where it was 29, 27, 33 and 6 for group BA, BB, BC, and BD respectively when the tensile steel reinforcement ρ/pb was 0.18 while it was 2, 28, 53, and 42 for group BA, BB, BC, and BD respectively when the longitudinal reinforcement ρ/pb was 0.28. Shear is primarily resisted by shear stresses in the concrete up to the cracking load. Shear is resisted after cracking by aggregate interlock, the main reinforcing bars' dowel action, and the resistance of the remaining untracked concrete at the beam's upper part[27]. The proportion carried by aggregate interlock is highly influenced by the crack's surface roughness and the degree of displacement (opening). The failure surfaces of the beams in this study were significantly smoother at higher concrete strengths, showing that the shear force carried by aggregate interlock reduces with an increase in concrete compressive strength from 45 MPa to 65 MPa. The reason can be explained as follows. The stiffness of concrete matrix when the concrete compressive strength is high will be greater than the stiffness of the gravel. Therefore, the crack can find its way easily through the gravel instead of moving around it. This makes the shear crack surface smoother than the honey-comb surface for the case of low concrete compressive strength. Interlocking aggregates has long been thought to be the most important factor providing in reinforced concrete beam shear strength. In other words, when shear stress exceeds capacity of aggregate interlock in reinforced concrete beams, shear failure occurs. The size effect in reinforced concrete beams is traditionally described by the reduced aggregate interlock capacity in deeper slender beams due to the larger critical crack, as previously mentioned. Shear displacement along the crack is resisted in part by the longitudinal steel's dowel action, resulting

in vertical tension in the surrounding concrete. The tensile strength of concrete is usually related to concrete compressive strength. The shear force that untracked concrete can withstand is also affected by concrete compressive strength and the size of the compression zone above the crack. These shear transmission mechanisms are interconnected and difficult to separate. Any weakness in one will impact the other two, and which one fails first to induce beam failure will be determined by the relative magnitudes of the forces carried by each, as well as the resistance. The aggregate interlock is the first mechanism to fail in beams with higher concrete strengths, requiring dowel action and shear in the compression zone to resist further shear forces. There are two types of failure. A sudden and occasionally explosive failure occurs when the state of stress meets the failure criterion for the concrete in the compression zone. Vertical tension in the concrete surrounding the bars creates splitting cracks along with the reinforcement if dowel resistance is managed. In this work, both forms of failure were reported.

Table 5: Cracking and ultimate load increasing percentage per different concrete strengths

Specimen	Pcr (kN)	Pc %	Pu (kN)	Pu %
BA75*150-45-(3-8) *	20.93	1	33.44	1
BA75*150-65-(3-8)	22.54	1.08	43.23	1.29
BA75*150-45-(4-8) *	25.52	1	45.48	1
BA75*150-65-(4-8)	27.64	1.08	46.52	1.02
BB100*200-45-(2-10) *	30.22	1	57.4	1
BB100*200-65-(2-10)	32.8	1.09	73.17	1.27
BB100*200-45-(3-10) *	35.44	1	65.45	1
BB100*200-65-(3-10)	37.04	1.05	83.94	1.28
BC125*250-45-(2-12) *	40.41	1	87.25	1
BC125*250-65-(2-12)	45.65	1.13	120.08	1.38
BC125*250-45-(3-12) *	48.6	1	102.56	1
BC125*250-65-(3-12)	66.1	1.36	157.28	1.53
BD150*300-45-(2-16) *	70.2	1	161.16	1
BD150*300-65-(2-16)	95.3	1.36	171.22	1.06
BD150*300-45-(3-16) *	100.02	1	200.5	1
BD150*300-65-(3-16)	125.4	1.25	285.1	1.42

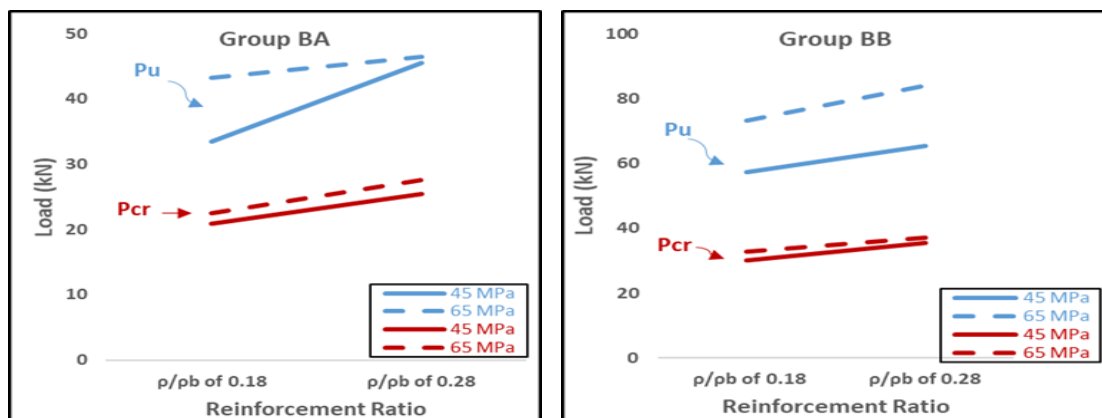
* Reference beam to compare

10.5 Influence of Longitudinal Steel Ratio on Cracking and Ultimate Capacity

The effect of the longitudinal reinforcement ratio on the capacity of visible cracking load Pcr and ultimate load Pu for all tested beams with constant concrete compressive strength (45MPa and 65MPa) and the same cross-section (75*150mm, 100*200mm, 125*250mm and 150*300mm) is present in Figure 6.

The impact of the main reinforcement ratio on capacity of visible cracking load Pcr and ultimate load Pu is predominantly evident. It can be seen from the figure, for all concrete compressive strengths, increasing the main reinforcement steel ratio increases the capacity of visible cracking and ultimate loads in each group for all beam specimens.

Table 6 shows the increasing percentage of the visible cracking and ultimate loads for different longitudinal reinforcement ratios with constant cross-section sizes (75*150mm, 100*200mm, 125*250mm and 150*300mm) and the same concrete compressive strength (45MPa and 65MPa) for all tested beam specimens.



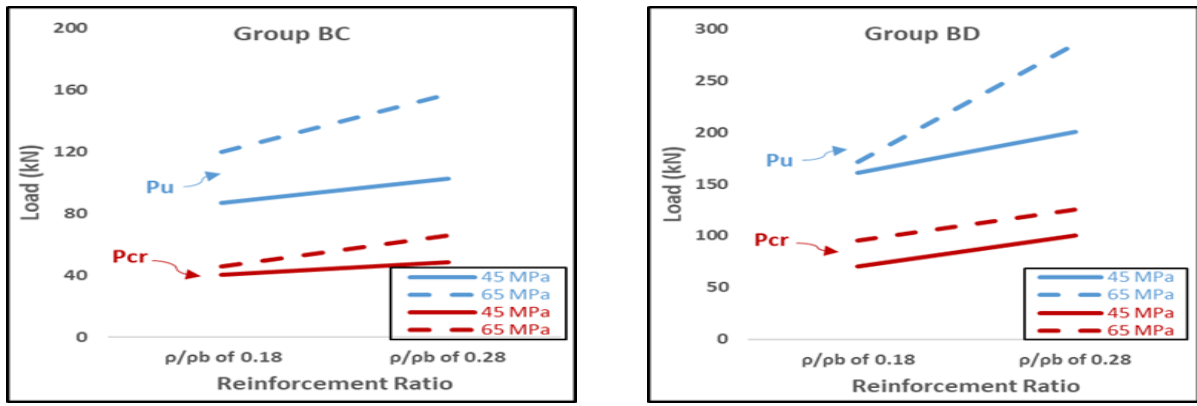


Figure 6: Capacity of cracking and ultimate loads with varying steel reinforcement ratios

Table 6: Cracking and ultimate load increasing percentage per different longitudinal reinforcement ratios

Specimen	Pcr (kN)	Pcr %	Pu (kN)	Pu %
BA75*150-45-(3-8) *	20.93	1	33.44	1
BA75*150-45-(4-8)	25.52	1.22	45.48	1.36
BA75*150-65-(3-8) *	22.54	1	43.23	1
BA75*150-65-(4-8)	27.64	1.23	46.52	1.08
BB100*200-45-(2-10) *	30.22	1	57.4	1
BB100*200-45-(3-10)	35.44	1.17	65.45	1.14
BB100*200-65-(2-10) *	32.8	1	73.17	1
BB100*200-65-(3-10)	37.04	1.13	83.94	1.15
BC125*250-45-(2-12) *	40.41	1	87.25	1
BC125*250-45-(3-12)	48.6	1.2	102.56	1.18
BC125*250-65-(2-12) *	45.65	1	120.08	1
BC125*250-65-(3-12)	66.1	1.45	157.28	1.31
BD150*300-45-(2-16) *	70.2	1	161.16	1
BD150*300-45-(3-16)	100.02	1.42	200.5	1.24
BD150*300-65-(2-16) *	95.3	1	171.22	1
BD150*300-65-(3-16)	125.4	1.32	285.1	1.67

* Reference beam to compare

Depending on the longitudinal steel reinforcement ratio used in each group showed in Table 6, it can be concluded that the ultimate failure load was significantly influenced by changing the steel reinforcement ρ/pb from 0.18 to 0.28 for all groups. The percentage of increases the ultimate load was 36,14,18 and 24 for group BA, BB, BC, and BD respectively when the concrete compressive strength is 45 MPa while it was 8, 15, 31, and 67 for group BA, BB, BC, and BD respectively when the concrete compressive strength is 65 MPa. This indicates that the beam with a lower flexural reinforcement ratio has lower post-diagonal cracking shear strength. Another conclusion is that the size of beam has an influence on the contribution of the dowel action to the ultimate shear strength. To focus light on this phenomenon it is preferable to eliminate the rule of aggregate interlock, so it is better to choose the case of concrete compressive strength $f_c = 65\text{MPa}$ since it has less effective aggregate interlock. A comparison between the beams of group BA, BB, BA, and BD (which have size 75*150mm, 100*200mm, 125*250mm and 150*300mm respectively), all for the case $f_c = 65\text{MPa}$, indicated that the share of dowel action in the ultimate shear strength increases as the size of beam increase as indicated in Table 6. This can be attracted to the fact that the principal shear crack takes a little longer time to fully developed in larger size beam than in a similar smaller size which allows to stronger action of the dowel bars to take place, and this eventually results in a higher ultimate shear capacity. The basic shear transfer mechanisms are pronounced influenced by the tensile steel reinforcement ratio. The magnitude of shear stresses at the crack's tip is a key variable that affects how quickly a flexural crack develops into an inclined one. The depth of penetration of the flexural crack determines the severity of the principal stresses above it's the tensile steel reinforcement ratio increased, the flexural crack penetrates will be reduced. The lower the flexural crack penetration, the lower the principal stresses for a given applied load, and therefore the higher the shear required generating the principal stresses that induce diagonal tension cracking. Increasing the longitudinal reinforcement ratio will increases the member's dowel capacity by increasing the dowel area and consequently reducing the tensile stresses induced in the surrounding concrete. The steel stress at the time of shear failure is shown to be a significant variable in determining the dowel force carried by the reinforcing bars, and hence the concrete beam's shear capacity. Increasing the longitudinal reinforcement ratio also affects the aggregate interlock capacity. Beams with ρ/pb of 0.18 longitudinal reinforcement will have wide, long cracks in contrast to the shorter, narrow cracks found in beams with ρ/pb of 0.28 longitudinal. Since the aggregate interlock mechanism depends on the crack width, an increase in the aggregate interlock force is to be expected with an increase in the longitudinal reinforcement ratio.

10.6 Load -Deflection Relationships

The Figures 7 to 14 shows the load-displacement history for the tested beams measured at the misspent. Before the appearance of the first flexural cracks, all beam specimen's showcased linear elastic behaviour followed by nonlinear behaviour up to the failure as indicated by the load-deflection relationships. Table 3 illustrates the failure load and mid-span deflection values of all tested RC beams. Centreline and corresponded to the bending moment diagram. As the shear span cracks grew longer, they transitioned from vertical flexural cracks to flexural-shear cracks. The sharp increase in deflection or the sudden decrease in applied load indicates the development of critical shear cracks in the load-misspent deflection curves. These curves show a short, straight segment after achieving the maximal shear capacity, and the applied load to the beams rapidly dropped after that. The test results show the brittle failure happened following the rapid drop in load with increasing crack width. The rate of development in the widths of existing cracks slowed significantly at this point, and all further deformation of the beam was largely because of the development of major diagonal web-shear cracks. Shear strength in beam specimens began to decline very soon after one or two diagonal cracks appeared. The deviation in such specimens, however, was not considerable.

10.7 Influence of Size on Load-deflection Curves

All beam specimens' load-misspent deflection curves are classified into four groups based on their cross-sectional size, as illustrated in Figures 8 to 10. The figures take the influence of size as a variable and keeping the concrete strength and the tensile steel reinforcement ratio as constant to isolate the member depth effectiveness. The applied load and the specimens' misspent deflection during the initial loading stage having linear relationships, as can be seen in the figures. Because the shear contribution of concrete increased with the increase in depth of the beam, the initial stiffness of each beam within the same set rose somewhat, as predicted, and was largely unaffected by the emergence of flexural cracks. In other words, the ultimate shear strength is proportional to the depth of the cross-section.

It can be seen from these Figures 9 and 10, except for beam specimen BA75*150-65-(4-8), increasing beam size has a significant influence on the deflection at the failure load. In another word, increasing beam depth from 150mm to 300mm has led to increasing the ultimate load besides decreasing their final deflection at the same level of load, which is the apparent size effect in the stiffness of the tested beams. It can be noted from these figures, beam specimen BA75*150-65-(4-8) shows the largest displacement value compared with all the other 15 tested beams because of its failure mode which is different from the other tested specimens consequently it is out of the comparison made.

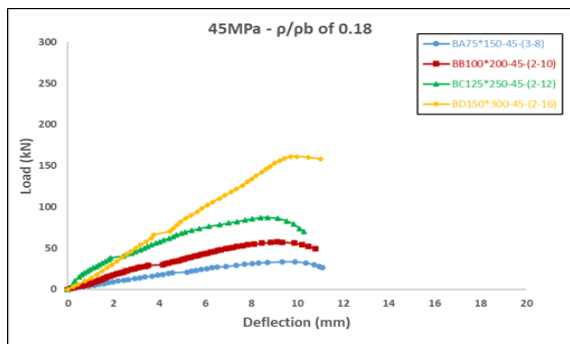


Figure 7: Load-misspent deflection relationship for different cross-sections size with 45 MPa compressive strength and ρ/pb of 0.18 tensile reinforcement

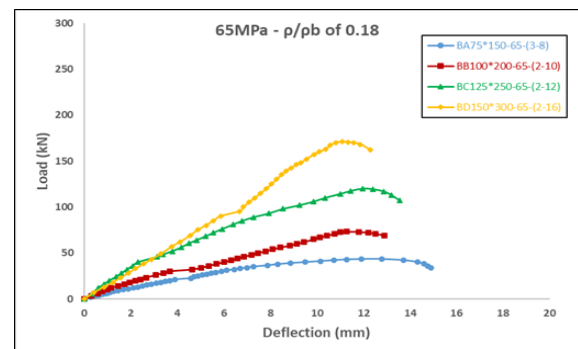


Figure 8: Load-misspent deflection relationship for different cross-sections size with 65 MPa compressive strength and $\rho/above$ 0.18 tensile reinforcement

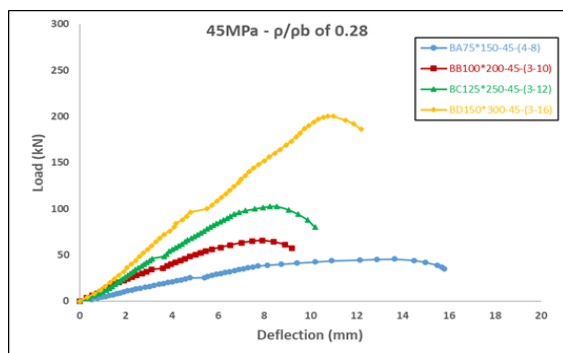


Figure 9: Load-midspan deflection relationship for different cross-sections size with 45 MPa compressive strength and ρ/pb of 0.28 tensile reinforcement

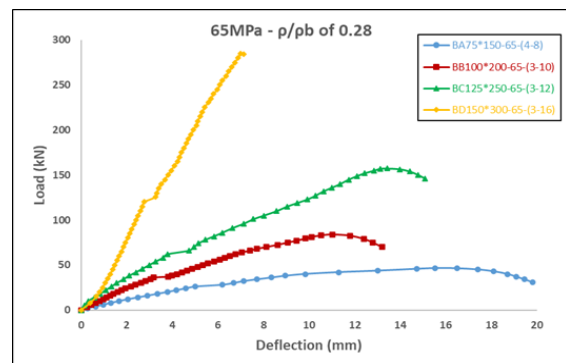


Figure 10: Load-misspent deflection relationship for different cross-sections size with 65 MPa compressive strength and $\rho/above$ 0.28 tensile reinforcement

10.8 Influence of Concrete Strength and Longitudinal Reinforcement Ratio Load-deflection Relationship

Figures 11 to 14 illustrates the influence of concrete compressive strength and the longitudinal reinforcement ratio on a load-misspent deflection for the reinforced concrete tested beams without stirrups. The slopes of the descending part of the load-misspent deflection relationship for high-strength concrete beams are sharper than those for normal-strength concrete beams, as can be seen in these figures. Shear is resisted after cracking by aggregate interlock, flexural reinforcing bars dowel action, and untracked concrete in the compression zone of the beam. The proportion carried by aggregate interlock is strongly dependent on the crack's surface roughness. The fracture surfaces were identical, and the surfaces of the crack were smooth, in concrete beams with 65 MPa compared with 45 MPa, showing that the shear force transmitted by aggregate interlock reduces with increasing concrete compressive strength. It is shown from these figures that beam capacity increases significantly as the ratio of longitudinal reinforcement increases.

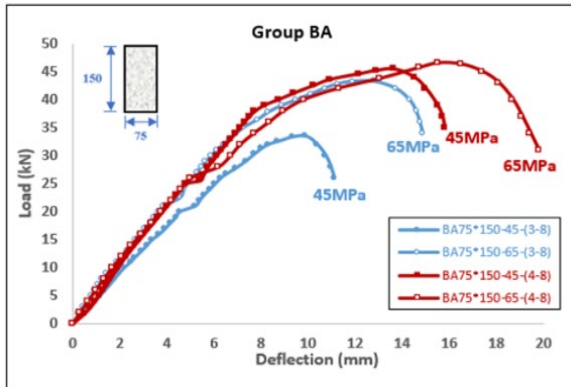


Figure 11: Load-misspent deflection relationship for group BA

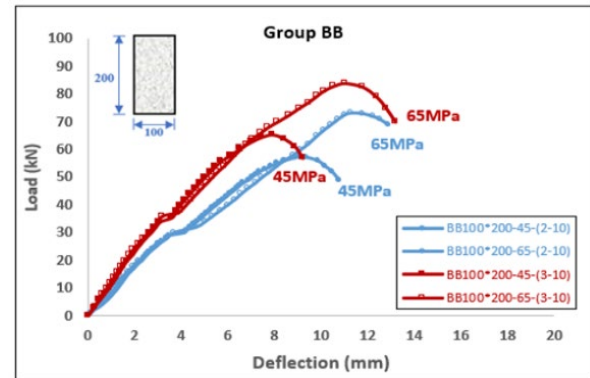


Figure 12: Load-misspent deflection relationship for group BB

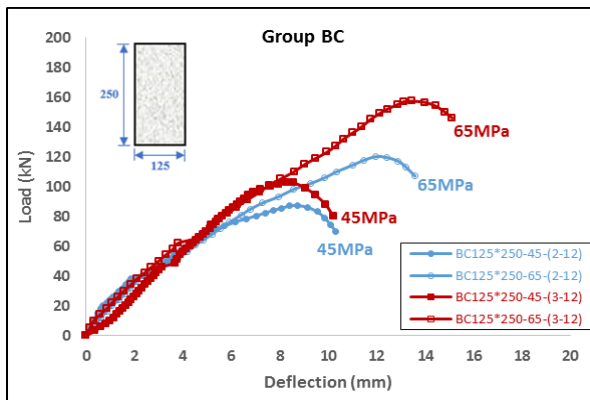


Figure 13: Load-misspent deflection relationship for group BC

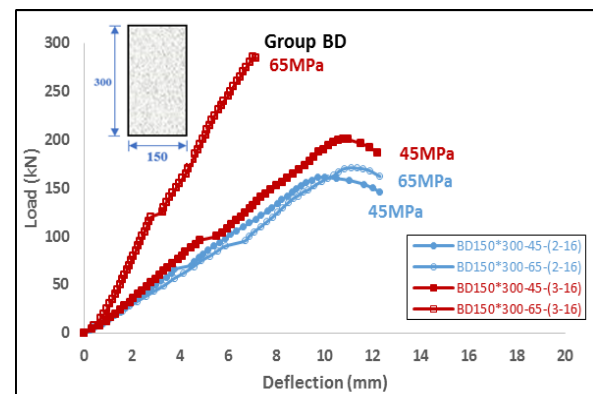


Figure 14: Load-misspent deflection relationship for group BD

11. Conclusions

The experimental study presented in this paper was mainly concerned to examine the structural behavior and load-carrying capacity of reinforced concrete beams with different rectangular cross-sections under shear failure. The experimental results for the tested beams showed that:

- 1) All of the tested beam specimens failed in shear except one which had failed by the crushing of the compression zone at mid-span.
- 2) The size influence on the reinforced concrete tested beams in terms of visible cracking and ultimate load were the more important variable from the concrete compressive strength or the main reinforcement ratio.
- 3) Increasing beam height from 150 to 250 mm has decreased the cracking and ultimate shear strength ratio for all groups except for group four when the beam height increased from 150 to 300 mm the cracking and ultimate shear strength ratio has increased. In other words, the behavior of the group four is different than other groups in terms of increasing beam depth on the shear capacity.
- 4) Increasing beam height from 150 to 250 mm has decreased the cracking and ultimate shear strength ratio. The percentage of decreasing was 34, 61 for concrete compressive strength of 45MPa with longitudinal reinforcement ratio to balance reinforcement ratio of 0.18 and it was 48, 0 for concrete compressive strength of 65MPa with longitudinal reinforcement ratio to balance reinforcement ratio of 0.18, and finally it was 191, 188 for concrete compressive strength of 45MPa with longitudinal reinforcement ratio to balance reinforcement ratio of 0.18.

- 5) Increasing beam height from 150 to 300 mm has increased the cracking and ultimate shear strength ratio. The percentage of increasing was 205, and 102 for concrete compressive strength of 45MPa and 65MPa with longitudinal reinforcement ratio to balance reinforcement ratio of 0.18 and 0.28.
- 6) Increasing the concrete compressive strength from 45 MPa to 65 MPa, increases the ultimate shear strength for all groups. The percentage of increase was 29, 27, 33 and 6 for the fourth groups respectively when the longitudinal reinforcement ratio to balance reinforcement ratio was 0.18 while it was 2, 28, 53, and 42 for the fourth groups respectively when the longitudinal reinforcement ratio to balance reinforcement ratio was 0.28.
- 7) The ultimate failure load was significantly influenced by changing the longitudinal reinforcement ratio to balance reinforcement ratio from 0.18 to 0.28 for all groups. The percentage of increases the ultimate load was 36, 14, 18 and 24 for the fourth groups respectively when the concrete compressive strength is 45 MPa while it was 8, 15, 31, and 67 for the fourth groups respectively when the concrete compressive strength is 65 MPa.
- 8) The initial stiffness of each beam increased somewhat within the same set, as predicted. In other words, the ultimate shear strength is proportional to the depth of the cross-section.
- 9) Increasing beam depth from 150mm to 300mm has led to increasing the ultimate load besides decreasing their final deflection at the same level of load, which is the apparent size effect in the stiffness of the tested beams.

Author contribution

All authors contributed equally to this work.

Funding

This research received no specific grant from any funding agency in the public, commercial, or not-for-profit sectors.

Data availability statement

The data that support the findings of this study are available on request from the corresponding author.

Conflicts of interest

The authors declare that there is no conflict of interest.

References

- [1] P.-C. Aïtcin, High-Performance Concrete E FN SPON. (2004).
- [2] [E. C. P. ASBL, Commentary Eurocode 2. European Concrete Platform ASBL, (2008).
- [3] S. Cholostiakow, M. Di Benedetti, K. Pilakoutas, and M. Guadagnini, Effect of beam depth on shear behavior of FRP RC beams, *J. Compos. Constr.*, 23 (2018) 40. [https://doi.org/10.1061/\(ASCE\)CC.1943-5614.0000914](https://doi.org/10.1061/(ASCE)CC.1943-5614.0000914)
- [4] D. Y. Yoo and J. M. Yang, Effects of stirrup, steel fiber, and beam size on shear behavior of high-strength concrete beams, *Cem. Concr. Compos.*, 87 (2018) 137–148. <https://doi.org/10.1016/j.cemconcomp.2017.12.010>
- [5] J.-Y. Lee, J.-H. Lee, D. H. Lee, S.-J. Hong, and H.-Y. Kim, Practicability of large-scale reinforced concrete beams using grade 80 stirrups, *ACI Struct. J.*, 115 (2018) 269–280.
- [6] A. Althin and M. Lippe, Size effects in shear force design of concrete beams, MSc Thesis, Division Struct, Eng. Fac. Eng., 70 (2018).
- [7] D. I. Shin, M. Haroon, C. Kim, B. S. Lee, and J. Y. Lee, Shear strength reduction of large-scale reinforced concrete beams with high-strength stirrups, *ACI Struct. J.*, 116 (2019) 161–172. <https://doi.org/10.14359/51716759>
- [8] G. B. Jumaa and A. R. Yousif, Size effect in shear failure of high strength concrete beams without stirrup reinforced with basalt FRP bars, *KSCE. J. Civ. Eng.*, 23 (2019) 1636–1650. <https://doi.org/10.1016/j.conbuildmat.2019.03.076>
- [9] T. Wu, H. Wei, and X. Liu, Shear behavior of large-scale deep beams with lightweight-aggregate concrete, *ACI Struct. J.*, 117 (2020) 75–89. <http://dx.doi.org/10.14359/51718009>
- [10] S. H. Chao, Size effect on ultimate shear strength of steel fiber-reinforced concrete slender beams, *ACI Struct. J.*, 117 (2020) 145–158. <http://dx.doi.org/10.14359/51718018>
- [11] No. 5/1984, Iraqi Specification, Portland Cement. Ministry of Planning, Central Agency for Standardization and Quality Control, (1984).
- [12] H. P. J. Taylor, Shear strength of large beams, *J. Struct. Div. ASCE.*, 98 (1972) 2473–2489.
- [13] ASTM C-494/C 494M, Standard specification for chemical admixtures for concrete, (2001).
- [14] ASTM C 1240 – 05, Standard specification for silica fume used in cementitious mixtures, (2005).
- [15] ASTM A615-16, Standard specification for deformed and plain carbon structural steel bars for concrete reinforcement. Annual Book of ASTM Standards, (2016).

- [16] ASTM C 39/C 39M – 03, Standard test method for compressive strength of cylindrical concrete specimens. (2003).
- [17] ACI 318M-19, Building code requirements for structural concrete and commentary, (2019).
- [18] ASTM C 192/C 192M-05, Standard practice for making and curing concrete test specimens in the laboratory. Annual Book of ASTM Standards, (2005).
- [19] TML Company, Strain gauges user guide, No Title, Tokyo Sokki Kenkyujo Co., Ltd, Japan, Web site www.tml.jp/e.
- [20] L. H. Sneed and J. A. Ramirez, Influence of effective depth on shear strength of concrete beams-experimental study, *ACI Struct. J.*, 107 (2010) 554–562.
- [21] Z. P. Bazant and M. T. Kazemi, Size effect on diagonal shear failure of beams without stirrups, *ACI Struct. J.*, 88 (1991) 268–276.
- [22] P. Bazant, Z. P.; Kim, J. K.; and Pfeiffer, Determination of nonlinear fracture parameters from size effect tests. (1984).
- [23] ACI-ASCE Committee 445R, Recent approaches to shear design of structural concrete, *ACI*, 55, (1999).
- [24] Shioya et al., Shear strength of large reinforced concrete beams, *ACI Struct. J.*, 118 (1990) 259–280.
- [25] D. Collins, M. P., and Mitchell, *Prestressed concrete structures*. Response Publications, Canada, (1997).
- [26] T. Sherwood and A. Lubell, Safe shear design of large, wide beams adding shear reinforcement is recommended, *Concr. Int. Des. Constr.*, (2004) 66–78.
- [27] ASCE-ACI Committee 426, The shear strength of reinforced concrete members, *J. Struct. Div.*, 99 (1973) 1091–1187.